https://doi.org/10.15255/KUI.2021.094
KUI-46/2022
Original scientific paper
Received December 30, 2021
Accepted March 19, 2022

Gas Holdup in Turbulent Bed Contactor: Experiments and Prediction Model

B. Bensebia,[a*] *F. Z. Chaouche*,[a] and *S. K. Moustefai*[b]

[a] Laboratory of "Plant Chemistry-Water-Energy", Department of Process Engineering, Faculty of Technology, Hassiba Benbouali University, B.P. 151, 02 000 Chlef, Algeria
[b] Department of Process Engineering, Faculty of Technology, Hassiba Benbouali University, B.P. 151, 02 000 Chlef, Algeria

Abstract

Knowledge of gas holdup is important for the development of the three-phase fluidized bed reactors. This work concerns the study of the effect of different operating conditions on gas retention in a turbulent bed contactor type 2 (TBC), such as superficial gas and liquid velocities, liquid to gas mass flows ratio (*L*/*G*), particle diameter and density, static bed height and free-open area of the supporting grid. The influence of the free area of the packing support grid (φ) on gas holdup was demonstrated and proved. The gas holdup increased to 22.92 % when φ decreased from 0.82 to 0.32. The experimental data (1746) led to the development of two correlations to predict gas holdup, one of which incorporated the ratio (*L*/*G*) which is an important design factor for gas-liquid contactors. The predicted results of holdup gas were in good agreement with the experimental data.

Keywords

Turbulent bed contactor, gas holdup, pressure drop, supporting grid, prediction model

1 Introduction

The turbulent bed contactor (TBC) is a gas-liquid contactor which offers new ways and solutions, particularly in the fields of reduction of air pollution,[1] humidification and dehumidification, biological processing, air-cooling, and particulate removal.[2]

TBC are three-phase fluidized beds in which the liquid is sprayed downward over the bed and flows downward by gravity through an expanded bed of solid packing supported by the upflowing continuous gas phase. The highly turbulent motion of the particles creates fast interface renewal and a large interfacial area, which in turn enhances the mass and heat transfer rates. This contacting device has many advantages over a conventional contactor, namely, a higher capacity and a higher efficiency.

O'Neil et al.[3] demonstrated that the turbulent bed contactor can operate in one of the following two hydrodynamic regimes: i) fluidization without flooding, and ii) fluidization due to incipient flooding. These two operating modes, respectively: Type 1 TBC and Type 2 TBC, depend on the density of the packing.

The gas holdup is one of the most important hydrodynamic and design parameters for the TBC.[4,5]

The information available in literature regarding gas holdup in TBC is relatively limited, and the most recent articles,[6–11] which use numerical simulation and CFD or even artificial intelligence, and which are devoted to the study of the hydrodynamics of the TBC, are only focused on pressure drops and bed expansion.

Gel'perin et al.[12] conducted the earliest studies of gas holdup using heavy particles and with grids of small open areas. A study carried by *Balabekov et al*.[13] showed that, at a constant gas velocity, the gas holdup was practically independent of liquid velocity, but when the gas velocity increased the gas holdup increased. The authors proposed an equation to determine the gas retention when liquid retention and expanded bed height are known. *Kito et al*.[14] showed that the gas holdup is practically independent of the viscosity of the liquid, the static bed height, and the packing density. For both operating regimes in TBC (types 1 and 2 TBC) and for partially and fully fluidized beds, empirical correlations for gas holdup were proposed by *Vunjak-Novakovic et al*.[15] The study conducted in a single TBC stage by *Soundarajan* and *Krishnaiah*[16] showed that the gas holdup is practically independent of the velocity of the liquid, free open area, particle density, and static bed height for the type 1 and type 2 operations.

For the gas-liquid-solid fluidized bed, various methods of measurement of the gas holdup were described by *Fan*.[17] Among the non-invasive techniques, the manometric method is one of the most used. It is more interesting to try to estimate the gas retention from experimental data that are easy to determine, such as pressure drop and bed expansion.

Generally, the data of pressure drop measured over the whole height of the column allows estimation of the gas holdup through the fluidized bed by manometric method,[18] *i.e.*, those including pressure drops through the fluidized bed and those across the supporting grid, while assuming that the pressure drops across the supporting grid are negligible.[12] Nevertheless, this assumption is not always correct, especially for relatively high gas velocities. *Bensebia et al*.[18] reported that the pressure drops of the supporting grid can represent up to 30 % of the total pressure

* Corresponding author: Assoc. Prof. Bensaber Bensebia
Email: bensebiab@yahoo.fr

drops. It would thus be reasonable to assume that certain inconsistencies noted in the results of the determination of the gas holdup, estimated using the pressure loss profile, were caused mainly by the omission of the pressure losses caused by the pressure grid support.

The aim of this work was to (i) study the gas holdup characteristics of a turbulent bed contactor (Type 2-TBC) across large variation intervals for operating conditions, (ii) try to explain the discrepancies noted by some authors' work between the experimental and the estimated gas holdup, when the experimental method of their determination was based on the profiles of pressure drop. Furthermore, using the experimental data and statistical analysis, two correlations were developed to predict gas holdup in the type-2 TBC.

2 Material and methods

2.1 Experimental procedure and apparatus

The experimental setup (Fig.1) consisted mainly of a Plexiglas column of 0.12 m inside diameter with a total height of 1.60 m. Water was admitted to the bed through a distributor specially designed for this work,[18] which gave a uniform liquid distribution over the top of the bed. The air from a compressor passed through a pressure reducer before being injected into the gas distribution system at the bottom of the fluidization section. The liquid from the tray was pumped with a centrifugal pump to the liquid distributor, placed on top of the fluidizing section. The bed of particles consisted of polypropylene and hollow spheres that laid in the static state on a support grid, and placed at different openings to the inlet of the fluidizing section. The liquid and gas flow were measured by appropriated rotameters, and their rates were controlled by valves. The pressure drop through the column was measured using a U-tube water manometer.

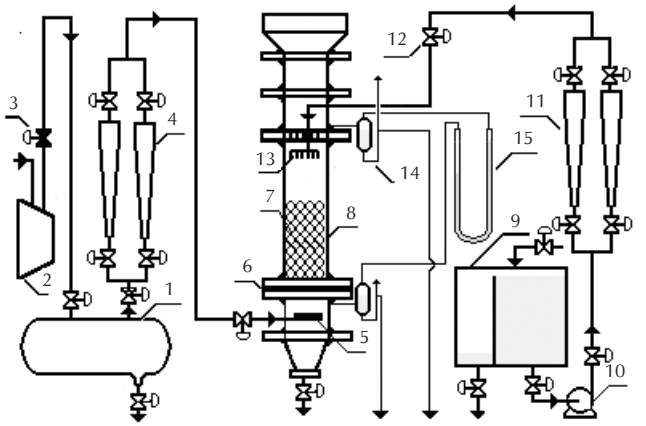

1. Gas tank
2. Compressor
3. Valve reducer
4. Gas rotameter
5. Gas distributor
6. Packing grid
7. Packing
8. Column
9. Water tank
10. Water pump
11. Liquid rotameter
12. Liquid valve
13. Liquid distributor
14. Fluctuation reducer
15. U-Manometer

Fig. 1 – Experimental setup

2.2 Experimental conditions

The operating conditions are summarized in Table 1. Two packings (P_I and P_{II}) were used. The operating conditions for each experimental system were described previously[18] for each experimental system. In this study, the gas flow rate (G) was varied (G) between 0 and 10 kg m^{-2} s^{-1}, and the liquid flow rates were: 4.57, 10.23, 15.84, 20.94, and 27.90 kg m^{-2} s^{-1}. The pressure drop was measured by U-manometer, and the dynamic bed height was measured visually.[18]

2.3 Methods

2.3.1 Determination of gas holdup from column pressure drop measurement

For the fluidized bed section, the gas holdup in TBC can be expressed as:

$$\varepsilon_g = \frac{V_g}{V_d} \tag{1}$$

Assuming that the fluidized bed volume is the sum of the volumes of the different phases:

$$V_d = V_p + V_l + V_g \tag{2}$$

the following relationship among individual holdups can be written:

$$\varepsilon_p + \varepsilon_l + \varepsilon_g = 1 \tag{3}$$

Table 1 – Operating conditions

Packing		Static bed height (H_{st})/m	% Grid free open area (φ)	Liquid flux (L)/kg m^{-2} s^{-1}	Gas flux (G)/kg m^{-2} s^{-1}	Experimental systems
ρ_p/kg m^{-3}	d_p/m					
P_I: 868	0.010	0.09	32; 56; 82	4.57; 10.23; 15.84; 20.94; 27.90	0 ÷ 10	I, II, III
		0.06	32; 56; 82			IV, V, VI
P_{II}: 736	0.015	0.12	32; 56; 82			VII, VIII, IX
		0.09	56			XI
		0.06	32; 56; 82			XIII, XIV, XV

From Eq. (3), we can write:

$$\varepsilon_g = 1-\left(\varepsilon_p + \varepsilon_l\right) \tag{4}$$

This is the basic equation to determine the gas holdup (ε_g), if we can determine the solid holdup (ε_p) and the liquid holdup (ε_l). These two parameters can be linked to easily accessible experimental data: pressure drop through the column ($-\Delta P_C$) and the bed expansion (H_d/H_{st}). Writing the conservation of the mass of the solid at static and fluidized state, we obtain:

$$\rho_p\left(1-\varepsilon_0\right)H_{st} = \rho_p\varepsilon_p H_d \tag{5}$$

which gives:

$$\varepsilon_p = \frac{\left(1-\varepsilon_0\right)}{\left(H_d / H_{st}\right)} \tag{6}$$

To determine the gas retention with the manometric method using the experimental data on the pressure drop, it is suitable to write the general equation, which relates the liquid holdup (ε_l) to the pressure drop in the column.[18] The total pressure drop through the entire column ($-\Delta P_c$), consists of the sum of two terms.[12,14,18,19]

$$\left(-\Delta P_c\right) = \left(-\Delta P_b\right) + \sum\left(-\Delta P_f\right) \tag{7}$$

where ($-\Delta P_b$) represents the pressure drop in the fluidized bed due to the weight of the solid, liquid and gas phases, and ($\sum(-\Delta P_f)$) is the sum of all the pressure drops other than those mentioned above, these are the pressure drops due to the flow of gas through the supporting grid, the spray section above the bed, the friction on the walls of the column, and the forces to overcome surface tension.[14,18,19,22–24]

According to *Wozniak*,[19] the pressure drop in a TBC can be determined by the following expression:

$$\left(-\Delta P_b\right) = \left[\left(\rho_p\varepsilon_p\right) + \left(\rho_l\varepsilon_l\right) + \left(\rho_g\varepsilon_g\right)\right] g H_d \tag{8}$$

When the density of the gas is negligible compared to that of the liquid and the packing, Eqs. (8) and (7) can be simplified to Eq. (9):

$$\left(-\Delta P_c\right) = \left[\left(\rho_p\varepsilon_p\right) + \left(\rho_l\varepsilon_l\right)\right] g H_d + \sum\left(-\Delta P_f\right) \tag{9}$$

When ε_p is replaced by ε_0 (according to Eq. (6), which is more readily available, and considering Eqs. (4) and (5), we can write:

$$\varepsilon_g = 1-\left(\frac{H_{st}}{H_d}\right)\left[\left(1-\varepsilon_0\right) + \frac{\left[\left(-\Delta P_c\right) - \left(\sum\left(-\Delta P_f\right)\right)\right] - \rho_p\left(1-\varepsilon_0\right) g\ H_{st}}{\rho_l\ g\ H_{st}}\right] \tag{10}$$

The use of this equation requires knowledge of the fraction of the static bed voidage ε_0, the dynamic bed height H_d, and experimental data on total pressure drop ($-\Delta P_c$). To use Eq. (10), it is necessary to know the pressure drops (($-\Delta P_f$)), these are not always possible to neglect, especially for high superficial gas velocities; which is precisely the case for the TBC.

2.3.2 Determination of pressure drop $\sum(-\Delta P_f)$

Many authors[18,20–25] have observed that these contributions could constitute an important part of the total pressure drop through the column. Based on their results, we can write:

$$\sum\left(-\Delta P_f\right) = \left(-\Delta P_{g_r}\right) + \left(-\Delta P_\sigma\right) + \left(-\Delta P_w\right) \tag{11}$$

where ($-\Delta P_{gr}$), ($-\Delta P_w$), and ($-\Delta P_\sigma$), represent, respectively, the pressure drops due to the flow through the supporting grid, the gas friction against the walls of the column, and the gas-liquid surface tension.

Using the works of many authors,[12,14,18,20,25–31] devoted to these pressure drops, we obtained the following relation:

$$\sum\left(-\Delta P_f\right) = \left(0.98\ \mathrm{L}\left(1-\varphi\right)\left(\mathrm{Re}_b^{0.25} + 1.2\ m^{0.5}\right)\right) + \left(1.9\,\frac{1}{2}\left(\frac{u_g}{\varphi}\right)^2 \rho_g\right) + \left(\frac{4\sigma}{d_0}\right) \tag{12}$$

where the dimensionless Re_b is obtained by the following relation:[24]

$$\mathrm{Re}_b = \left(g / \left(m^{1.5}\gamma_l^{0.5}\right)\right) \tag{13}$$

is a dimensionless group considering a specific gas flow rate $m = U_g/h_1$ (m in s^{-1}), γ_l is the kinematic viscosity of the liquid in $\mathrm{m^2\,s^{-1}}$, and $h_1 = (\rho_L/L)(1-\varphi)$ is the height of the liquid layer held up on the supporting grid[24] (in m).

3 Results and discussion

3.1 Pressure drop and bed expansion

Fig. (2) shows the experimental data of the total pressure drop through the column. For all our experimental results,

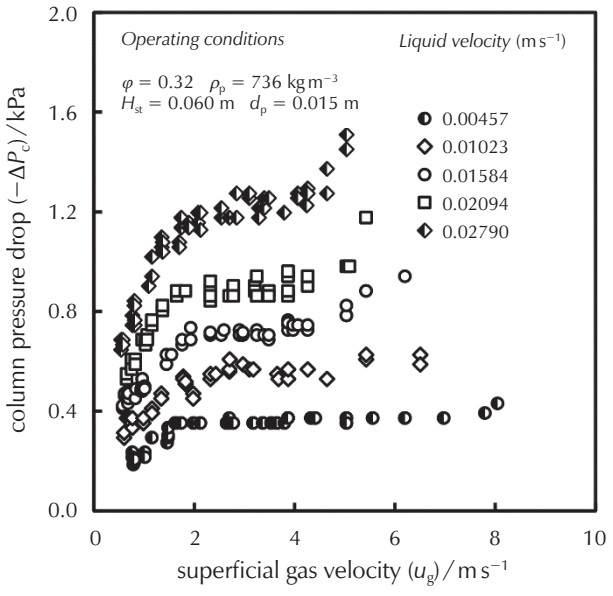

Fig. 2 – Variation of pressure drop ($-\Delta P_{cexp}$) with superficial gas velocity for given superficial liquid velocities

we observed that the evolution of total pressure drop through the column with the different operating variables (u_g, φ, H_{st},) was similar to that reported by different authors.[12,13,21–35,27–37]

The variation of the expansion bed (H_d/H_{st}) with the gas superficial velocity (u_g) at constant liquid velocity (u_l) is presented in Fig. (3). For the example considered, and for all the systems studied, we observed the same trends as those reported by most of the authors, concerning the evolution of the expansion with the operating variables.[14,23,30–34]

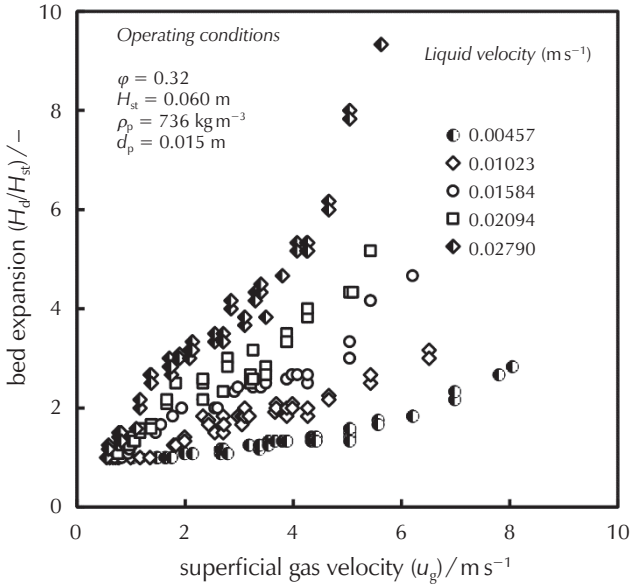

Fig. 3 – Variation of bed expansion (H_d/H_{st}) with superficial gas velocity for given superficial liquid velocities

3.2 Gas holdup

3.2.1 Effect of gas and liquid velocities on gas holdup

As may be deduced from Fig. (4), the gas holdup was strongly linked to the gas velocity and practically independent of the velocity of the liquid. In addition, at low gas velocities, the gas holdup increased monotonically with higher values of the slope. These results were comparable to those mentioned by many authors.[12,25,37]

As shown in Fig. (5), a slight variation of gas holdup with the superficial velocity of the liquid was observed at constant superficial gas velocity. This peculiarity was also noted by *Mbua Egbe*[39], who explained it by the increase in drops of liquid and the turbulence that this generated, thus causing an additional retention of gas.

In general, the increase in the flow of liquid, in the presence of support grids with relatively small opening, causes an increase in the expansion of the bed, which generates an increase in gas holdup.

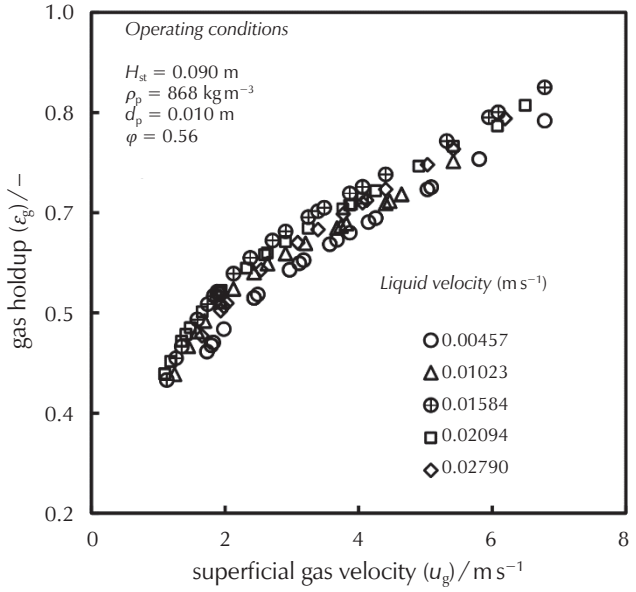

Fig. 4 – Effect of gas velocity on gas holdup at constant liquid velocity

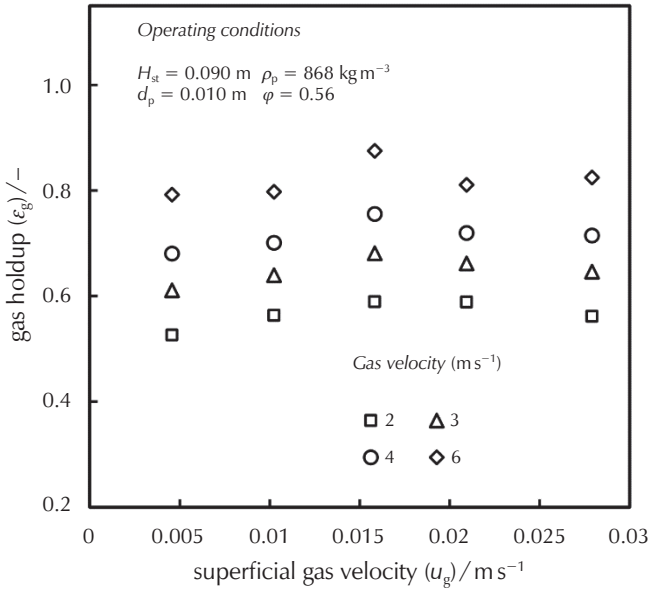

Fig. 5 – Effect of liquid velocity on gas holdup at constant gas velocity

3.2.2 Effect of free open area of supporting grid on gas holdup

As shown in Fig. (6), the gas holdup decreased significantly when the free open area of the supporting grid increased, and this effect was accentuated when the superficial gas velocity increased.

The assertions of the authors, concerning the effect of the free opening of the support grid, present disparities; thus, some authors[13,26] asserted that the gas retention was independent from the opening of the free opening of the support grid, and others[13,15] reported dependence. This

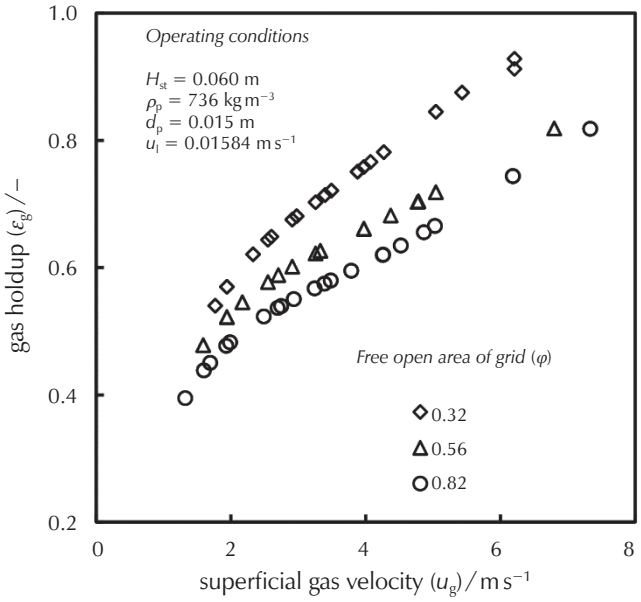

Fig. 6 – Effect of grid free open area (φ) on gas holdup

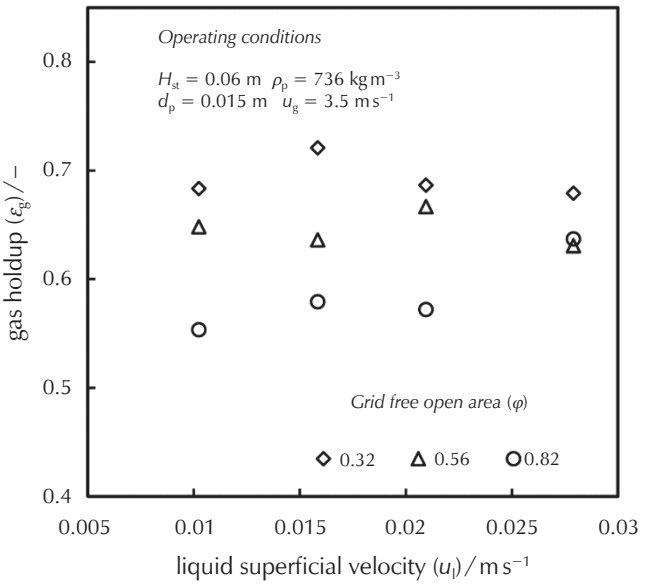

Fig. 7 – Effect of free open area of supporting grid (φ) on gas holdup for a given superficial liquid velocity

apparent contradiction can be explained by the fact that some of these authors used large opening support grids, while others used very small openings. Some authors have also worked with stagnant liquid.

The hydrodynamic behaviour of the fluidized bed was strongly affected by the free open area of the supporting grid; this was the result observed from a large number of experiments and with a wide range of variations in the opening of the support grids. According to *Gel'perin et al*.[12] and *Kito et al.*,[14,27,28,31] the hydrodynamic characteristics of TBC systems depend strongly on the opening of the packing supporting grid (φ).

In Fig. (7), the effect of the free opening area of the supporting grid on the gas holdup was reported. This figure shows that when the liquid flow increased, the effect of supporting grid decreased. In conclusion, it may be suggested that, as the free area of the support grid decreased, the dynamic height of the fluidized bed increased, which increased the volume fraction of the gas and led to increased gas retention. This conclusion was confirmed by Eq. (10).

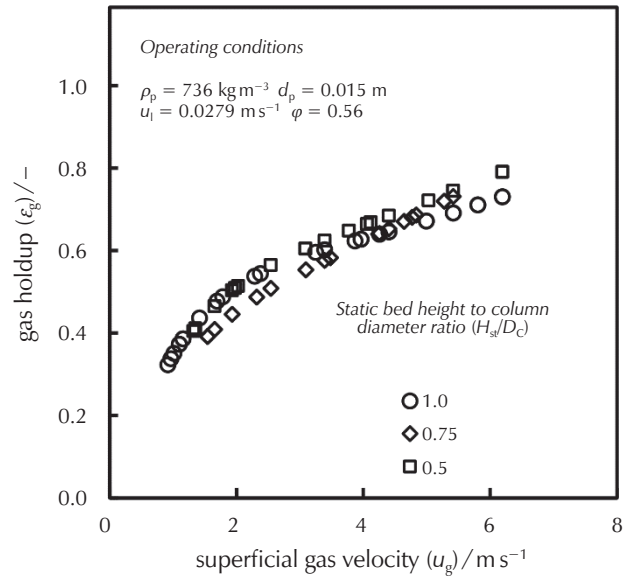

Fig. 8 – Effect of static bed height on gas holdup

3.2.3 Effect of static bed height to column diameter ratio on gas holdup

As shown in Fig. (8), there was practically no effect of the static bed height to column diameter ratio (H_{st}/D_C) on the gas holdup. These results were in accordance with those of other authors.[6,8]

3.2.4 Effect of liquid to gas mass flux ratio (L/G) on the gas holdup

The L/G ratio was an important design parameter of liquid-gas contactors, used to estimate the efficiency of mass and heat transfer operations.[38,39] It was therefore essential to study its evolution. Fig. (9) shows that, when the gas velocity was maintained constant, the gas holdup increased with the *L*/*G* ratio and decreased very significantly when the gas velocity decreased.

Fig. (10) shows that gas holdup increased when the (*L*/*G*) ratio decreased at constant superficial liquid velocity. However, this effect was attenuated when the superficial liquid velocity increased. In conclusion, to promote gas holdup, it would be preferable to operate with a low *L*/*G* ratio[38] and a moderate liquid flow rate.

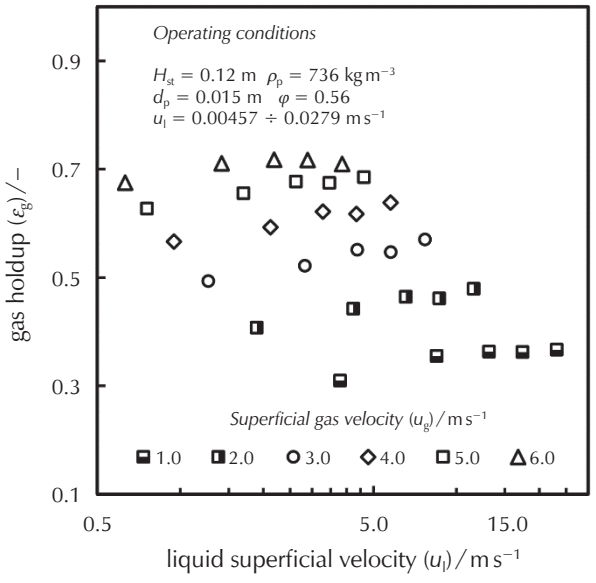

Fig. 9 – Effect of liquid to gas mass flow ratio (*L*/*G*) on gas holdup at constant gas velocity

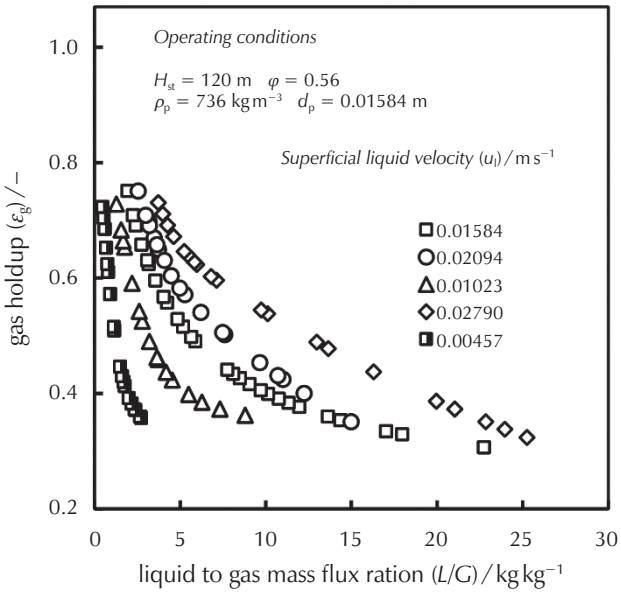

Fig. 10 – Effect of gas mass flow ratio (*L*/*G*) on gas holdup at constant liquid velocity

3.3 Prediction of gas holdup for the turbulent contact absorber (Type II TBC)

The variables on which the gas holdup may depend were: gas velocity (u_g), liquid velocity (u_l), density of gas (ρ_g), density of liquid (ρ_l), density of solid (ρ_p), particle size (d_p), static bed height (H_{st}), expanded bed height (H_d), free open area of supporting grid (φ), viscosity of gas (μ_g), viscosity of the liquid (μ_l), gas-liquid surface tension (σ), and gravitational constant (g). Therefore, if a theoretical relation exists between the gas holdup (ε_g), and the physical characteristic, and flow variables of the system, then ε_g may be written in the following form:

$$\varepsilon_g = f\left(u_g, u_l, \rho_g, \rho_l, \rho_p, d_p, D_c, H_{st}, H_d, \varphi, \mu_g, \mu_l, \sigma, g\right) \quad (19)$$

By considering the results of the analysis of the dependence of the gas holdup on the operating variables, and with the results of the dimensional analysis carried out, the adequate expression to estimate the gas holdup can be simplified to:

$$\varepsilon_g = f'\left(\left[\mathrm{Fr_g}\right]^a \left[\mathrm{Re_l}\right]^b \left[\varphi\right]^c\right) \quad (20)$$

The functional relationship between gas holdup and the dimensionless groups identified in Eq. (20), leads to Eq. (21), which gives a mean absolute percentage error value (MAPE) of 6.10 %.

$$\varepsilon_g = 0.203\ \mathrm{Fr_g}^{0.362}\ \mathrm{Re_l}^{0.039}\varphi^{-0.155} \quad (21)$$

We have also developed a correlation that incorporates the ratio (*L*/*G*), which was an important design factor for gas-liquid contactors:

$$\varepsilon_g = 0.276\ \mathrm{Fr_g}^{0.325}\left(\frac{L}{G}\right)^{-0.014}\varphi^{-0.137} \quad (22)$$

In Figs. (11) and (12) we have reported the experimental data of gas retention for all experimental points (1746 points) with the proposed correlations (Eqs. (21) and (22)).

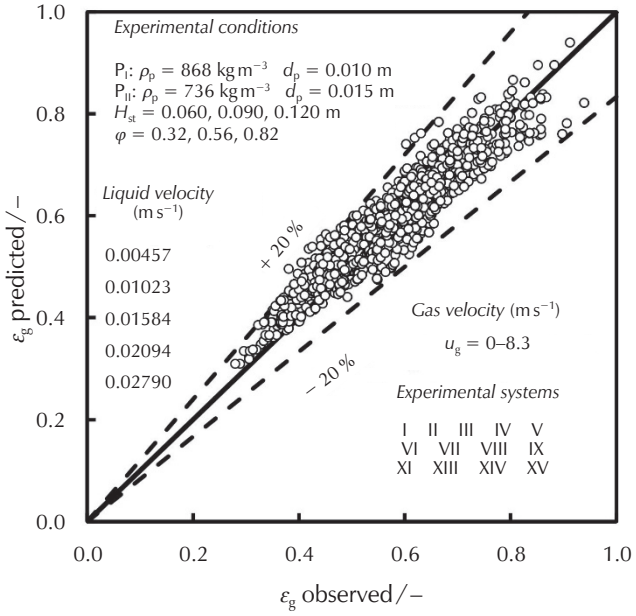

Fig. 11 – Comparison of gas holdup data with the proposed correlation (Eq. (21))

3.4 Comparison of gas holdup results with correlations

There are many empirical and semi-empirical correlations to predict gas retention. For the type II TBC, the equations used are summarized in Table (2).

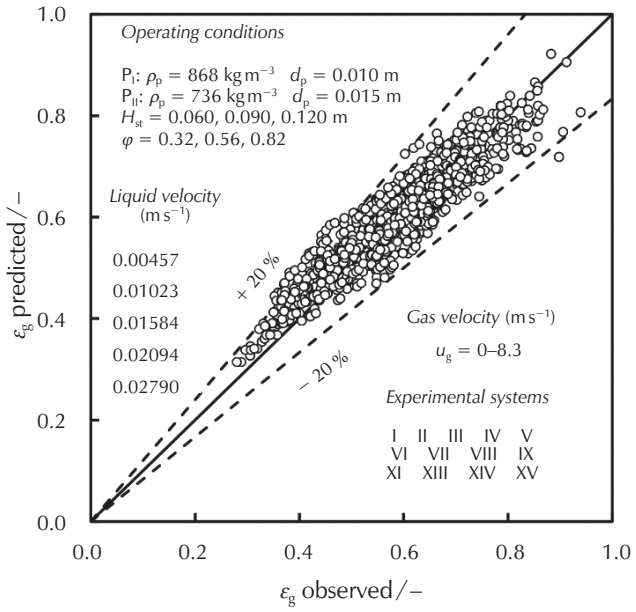

Fig. 12 – Comparison of gas holdup data with the proposed correlation (Eq. (22))

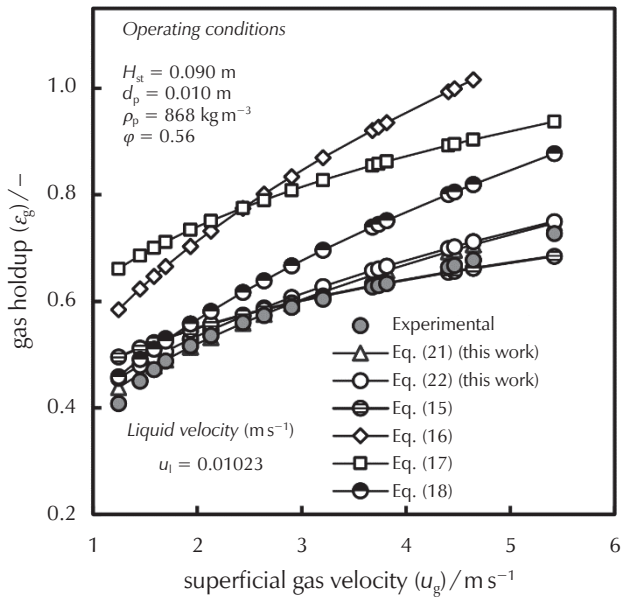

Fig. 13 – Comparison of gas holdup predictions based on various correlations

The results of this comparison (for the system II_2, as well as for all the other systems) for five different correlations (Eqs. (15)–(18)) are presented in Fig. 13, and show that there are three groups of correlations:

i. correlations which overestimate the gas holdup compared to the experimental data (Eqs (16) and (17)),
ii. correlations which moderately overestimate the predictions from a certain range of superficial gas velocity (Eq. (14) and (18));
iii. Eqs. (21) and (22) proposed in this work give the best results for predicting gas holdup. Eq. (15) of *Koundarajan & Krishnaiah*[16] also gives very satisfactory results for the prediction of our experimental data.

3.5 Models evaluation

An essential step in developing a predictive model was to evaluate the precision, accuracy, and reliability of the correlation deduced from this model. The precision of the predictive correlation was evaluated using the mean absolute percentage error (MAPE), the root mean square error (RMSE), the correlation coefficient (ρ_{XY}), and the explained variance (VEcv). The statistical indicators used were defined as follows:

$$\mathrm{MAPE}(\%) = \frac{100}{n}\sum_{i=1}^{n}\frac{\left|\varepsilon_{g_{(obs)_i}} - \varepsilon_{g_{(pred)_i}}\right|}{\varepsilon_{g_{(obs)_i}}} \qquad (23)$$

Table 2 – Correlations for estimating ε_g

Authors	Correlations for ε_g	Eqs.
Gel'perin et al.[12]	$\varepsilon_g = 0.93\left(\frac{d_p U_g' \rho_g}{\mu_g}\right)^{0.4}\left(\frac{d_p^3(\rho_p-\rho_g)\rho_g}{\mu_g^2}\right)^{-0.2}\left(U_g' = \frac{U_g}{1-\varepsilon_{l_{st}}(H_{st}/i_d)}\right)$	(14)
Soundarajan & Krishnaiah[16]	$\varepsilon_g = 0.322\ \mathrm{Fr}_g^{*0.22},\ \left(\mathrm{Fr}_g^* = (U_g/\varphi)/\sqrt{gd_p}\right)$	(15)
Kito et al.[14]	$\varepsilon_g = 0.19\left(\frac{d_p U_g^2 \rho_l}{\sigma}\right)^{0.11}\left(\frac{U_g}{\sqrt{gD_C}}\right)^{0.20}$	(16)
Vunjak-Novakovic et al.[15]	$\varepsilon_g = 0.628\ U_g^{0.237}$ (partial fluidization)	(17a)
	$\varepsilon_g = \frac{U_g}{U_{gmf}}\varepsilon_0 - 0.00443\left(\frac{H_{st}}{D_C}\right)^{0.433} d_p^{-0.494} L^{0.812}\left(\frac{\rho_p}{\rho_l}\right)^{0.090} - 0.02$ (full fluidization)	(17b)
Kito et al.[28]	$\varepsilon_g = 0.417\ U_g^{0.44}$	(18)

$$\mathrm{RMSE} = \sqrt{\sum_{i=1}^{n} \frac{1}{n}\left(\varepsilon_{g_{(obs)_i}} - \varepsilon_{g_{(pred)_i}}\right)^2} \quad (24)$$

$$\rho_{XY} = \frac{\sum_{i=1}^{n}\left(\varepsilon_{g_{(obs)_i}} - \overline{\varepsilon_{g_{(obs)}}}\right)\left(\varepsilon_{g_{(pred)_i}} - \overline{\varepsilon_{g_{(pred)}}}\right)}{\sqrt{\sum_{i=1}^{n}\left(\varepsilon_{g_{(obs)_i}} - \overline{\varepsilon_{g_{(obs)}}}\right)^2\left(\varepsilon_{g_{(pred)_i}} - \overline{\varepsilon_{g_{(pred)}}}\right)^2}} \quad (25)$$

$$\mathrm{VE_{CV}} = \left[1 - \frac{\sum_{i=1}^{n}\left(\varepsilon_{g_{(obs)_i}} - \varepsilon_{g_{(pred)_i}}\right)^2}{\sum_{i=1}^{n}\left(\varepsilon_{g_{(obs)_i}} - \overline{\varepsilon_{g_{(obs)}}}\right)^2}\right] 100\ \% \quad (26)$$

where $\varepsilon_{g_{(obs)_i}}$ and $\varepsilon_{g_{(pred)_i}}$ are, respectively, the i^{th} observed data and predicted values of gas holdup, among the n data, and $\overline{\varepsilon_{g_{(obs)}}}$ and $\overline{\varepsilon_{g_{(pred)}}}$ are, respectively, the mean of the observed data and of predicted values.

This evaluation was carried out to determine the predictive performances of the correlations developed in this study and those developed by other authors. The main results are presented in Table 3. The correlations proposed in this work gave the best results. In addition, the equations (Eq. (15)) proposed by *Soundarajan & Krishnaiah*[16] and to a lesser extent, (Eq. (18)), proposed by *Kito et al.*,[28] gave acceptable predictions.

To evaluate the reliability of the correlations considered in this work, we estimated the relative distribution of prediction results with errors (MAPE) less than 5, 10, 15, and 20 %. The results are shown in Table 4. For Eqs. (20) and (21) developed in this work, about 50 % of the results had an error of less than 5 %, and more than 98 % of predicted values had an error of less than 20 %. For the Eq. (15), proposed by *Soundarajan* and *Krishnaiah*,[16] 85.17 % of the predictions had a MAPE of less than 20 %. However, the other tested correlations were inadequate for predicting the gas holdup.

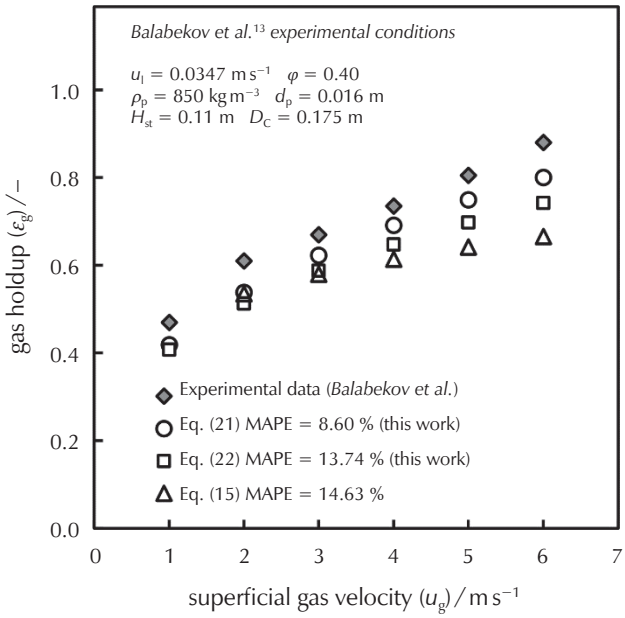

Fig. 14 – Plots of gas holdup (ε_g) *versus* superficial velocity (u_g) for *Balabekov et al.*[13] data

The applicability of the correlations developed in this work model was tested by using it with experimental data other than what was used in its development. The use of the correlations proposed in this work (Eqs. (21) and (22)) to correlate the data of *Balabekov et al.*[13], gave very satisfactory results (8.60 % for Eq. (21) and 13.34 % for Eq. (22)), as shown in Fig. 14. However, as a very limited amount of experimental data on gas holdup was available under the operating conditions of TBC-Type II, we were only able to correlate the results of *Balabekov et al.*[13] and those of *Abukhalifeh et al.*,[40] which also gave acceptable results (12.80 % for Eq. (21) and 13.21 % Eq. (22)). However, for the latter

Table 3 – Statistical results of the proposed correlations and those of other authors

Statistical function	Eq. (14) *Gel'perin et al.*[12]	Eq. (16) *Kito et al.*[14]	Eq. (17) *Vunjak-Novakovic et al.*[15]	Eq. (18) *Kito et al.*[27]	Eq. (15) *Soundarajan* and *Krishnaiah*[16]	Eq. (21) This work	Eq. (22) This work
MAPE / %	76.9	46.55	42.68	17.23	10.75	5.61	6.33
RMSE	0.4507	0.2710	0.2309	0.1124	0.0676	0.0384	0.0455
ρ_{XY}	0.88	0.91	0.91	0.91	0.85	0.95	0.93
VEcv / %	−1214.1	−375.3	−244.8	18.2	70.4	90.4	86.6

Table 4 – MAPE of prediction results by correlations

Percentage of predictions with a MAPE	*Soundarajan* and *Krishnaiah*[16] Eq. (15)	*Kito et al.*[31] Eq. (16)	*Vunjak-Novakovic et al.*[15] Eq. (17)	*Kito et al.*[28] Eq. (18)	This work	
					Eq. (21)	Eq. (22)
less than 20 %	85.17	0.23	6.64	61.25	98.83	98.63
less than 15 %	75.44	0.00	2.69	43.05	97.94	93.19
less than 10 %	56.90	0.00	1.43	29.42	86.15	77.90
less than 5 %	28.28	0.00	0.11	13.97	50.72	50.4
greater than 20 %	14.83	99.77	93.36	38.75	0.17	1.37

author, the density of the packing was 315 kg m^{-3}, which places the operating regime in Type 1-TBC.

The results obtained for the prediction of gas holdup using the proposed correlations from the different experimental systems of this study were very satisfying.

4 Conclusion

The experimental results determining the gas holdup in the fluidization regime of TBC-Type 2 showed that:

i. The gas holdup strongly depended on gas velocity;
ii. The gas holdup was practically independent of the liquid velocity. However, further analysis showed a slight variation;
iii. The gas holdup was not practically affected by the static bed height ;
iv. The gas holdup increased, obviously, with the reduction of the free area of the support grid, and this effect was more pronounced when the superficial gas velocity increased. Furthermore, the dependence of the gas holdup on the free area of the packing support grid (φ) was demonstrated and proved.
v. The prediction of gas holdup using the proposed correlations from the different experimental systems of this study and the data of *Balabekov et al.*[7] were very satisfying. The correlation proposed by *Soundarajan & Krishnaiah*[10] gave the best prediction of gas holdup for our experimental results. This was the only correlation that took into account the free opening area of the packing grid, and this result once again confirmed the relationship between the gas holdup and the free area of the support grid.

List of abbreviations and symbols

D_C – column inside diameter, m
d_p – packing diameter, m
Fr_g – gas Froude number $\left(G / \rho_g\right) / \sqrt{g d_p}$, dimensionless
Fr_l – liquid Froude number $\left(L / \rho_l\right) / \sqrt{g d_p}$, dimensionless
g – acceleration due to the gravity, m s^{-2}
G – mass flow rate of gas per unit area, kg m^{-2} s^{-1}
H_d – expanded bed height, m
h_l – height of liquid layer held up on the lower grid, m
H_{st} – static bed height, m
L – liquid mass flow rate per unit area, kg m^{-2} s^{-1}
m – specific gas flow rate $m = U_g/h_1$, s^{-1}
$-\Delta P_b$ – pressure drop in the bed, Pa
$-\Delta P_p$ – pressure drop due to dry packing, Pa
$-\Delta P_l$ – pressure drop due to the liquid in the bed, Pa
$-\Delta P_c$ – total pressure drop across the column, Pa
$\sum(-\Delta P_f)$ – all pressure drop other than those in the bed, Pa
$-\Delta P_d$ – dry grid and apparatus pressure drop, Pa
$-\Delta P_{gr}$ – pressure drop of flow through the lower grid, Pa
$-\Delta P_{hl}$ – pressure drop of the liquid held up by the grid, Pa
$-\Delta P_\sigma$ – pressure drop due to gas-liquid surface tension, Pa
$-\Delta P_w$ – pressure drop due to gas friction against walls, Pa
Re_b – dimensionless variable $\left(Re_b = \left(g / (m^{1.5}\gamma_l^{0.5})\right)\right)$, dimensionless
Re_l – liquid Reynolds number, $(\rho_l U_l d_p / \mu)$, dimensionless
U_g – superficial gas velocity, m s^{-1}
U_g^* – superficial gas velocity to free-open area (U_g / φ), m s^{-1}
U_l – superficial liquid velocity, m s^{-1}
V_d – volume of the dynamic (expanded) bed, m^3
V_g – volume of the gas phase in the bed, m^3
V_l – volume of the liquid phase in the bed, m^3
V_p – volume of the packing in the bed, m^3
We_l – Weber number $(d_p U_l^2 \rho_p / \sigma)$, dimensionless
γ_l – kinematic viscosity of the liquid, m^2 s^{-1}
ε_0 – voidage of the static bed without gas-liquid flow, m^3 m^{-3}
ε_g – gas holdup $(V_g/\Omega H_d)$, m^3 m^{-3}
ε_l – liquid holdup based on expanded bed $(V_l/\Omega H_d)$, m^3 m^{-3}
$\varepsilon_{l,st}$ – liquid holdup based on static bed $(V_l/\Omega H_{st})$, m^3 m^{-3}
ε_p – packing holdup based on expanded bed $(V_p/\Omega H_d)$, m^3 m^{-3}
φ – free-open area of the supporting grid, –
μ_g – dynamic viscosity of the gas, Pa s
μ_l – dynamic viscosity of the liquid, Pa s
Ω – cross-sectional area of the column $(\pi D_C^2/4)$, m^2
ρ_g – gas density, kg m^{-3}
ρ_l – liquid density, kg m^{-3}
ρ_p – packing density, kg m^{-3}
σ – gas-liquid surface tension, N m^{-1}
MAPE – mean absolute percentage error
RMSE – root mean square error
TBC – turbulent bed contactor
VEcv – explained variance
ρ_{XY} – correlation coefficient

References
Literatura

1. *S. Durga Jeevitha, A. Annam Renita, K. Soundarajan, K. Krishnaiah, J. Abbas Mohaideen,* A Review on the Potential of Turbulent Contact Absorber for Air Pollution Control, Int. J. Appl. Bioeng. **2** (1) (2008) 77–79, doi: https://doi.org/10.18000/ijabeg.10028.
2. *K. Muroyama, L.-S. Fan,* Fundamentals of Gas-Liquid-Solid Fluidization, AIChE J. **31** (1) (1985) 1–34, doi: https://doi.org/10.1002/aic.690310102.
3. *B. K. O'Neill, D. J. Nicklin, N. J. Morgan, L. S. Leung*, The hydrodynamics of gas–liquid contacting in tower with fluidized packing, Can. J. Chem. Eng. **50** (1972) 595–601, doi: https://doi.org/10.1002/cjce.5450500507.
4. *H. M. Jena, G. K. Roy,* Prediction of gas holdup in a three-

phase fluidized bed from bed pressure drop measurement, Chem. Eng. Res. Des. **86** (11) (2008) 1301–1308, doi: https://doi.org/10.1016/j.cherd.2008.05.007.

5. *H. M. Jena*, Hydrodynamics of Gas-Liquid-Solid Fluidized and Semi-Fluidized Beds, PhD Thesis, Department of Chemical Engineering, National Institute of Technology, Rourkela 769008, India, 15, 2009.
6. *H. Abu Khalifeh, M. Alkhedher, S. Fernandes,* Two Dimensional Computational Fluid Dynamics Simulations of Three-Phase Hydrodynamics in Turbulent Bed Contactor, Int. Rev. Model. Simul. **14** (4) (2021) doi: https://doi.org/10.15866/iremos.v14i4.20318.
7. *A. Ullah, A. Amanat, M. Imran, S. S. Gillani M. K. A. Khan*, Effect of turbulence modeling on hydrodynamics of a turbulent contact absorber, Chem. Eng. Process. **156** (2020) 108–101, doi: https://doi.org/10.1016/j.cep.2020.108101.
8. *M. Imran, A. Ullah, S. W. Ahmad, H. G. Qutab, M. Hameed*, Numerical Simulation of Hydrodynamics in a Turbulent Contact Absorber: A Simplified Approach, Arab. J. Sci. Eng. **45** (9) (2020) 7477–7485, doi: https://doi.org/10.1007/s13369-020-04605-4.
9. *H. Abu Khalifeh; M. Alkhedher, S. Fernandes*, A CFD Simulation for a Two-Phase Turbulent Bed Contactor, in: 8th International Conference on Modeling Simulation and Applied Optimization (ICMSAO), 15–17 April 2019, Bahrain pp. 1–4, doi: https://doi.org/10.1109/ICMSAO.2019.8880361.
10. *S. S. J. Gillani, A. Ullah, M. Zaman, I. R. Chugtai, M. H. Inayat*, Counter-current three-phase fluidization in a turbulent contact absorber: A CFD simulation, Particuology **35** (2017) 51–67, doi: https://doi.org/10.1016/j.partic.2016.10.008.
11. *K. Wang, L. W. Zhang, L. K. Huang*, Numerical Study on Air Flow with Various Accuracy Conditions in a Turbulent Contact Absorber, in: 2nd International Conference on Bioinformatics and Biomedical Engineering (iCBBE2008), 16–17 May 2008, Shanghai, China, doi: https://doi.org/10.1109/ICBBE.2008.469.
12. *N. I. Gel'Perin, V. I. Savshenko, V. Z. Grishko*, Some Hydrodynamics Laws of Apparatus Packed with Fluidized spheres, Theor. Chem. Eng. **2** (1) (1968) 65–71.
13. *O. S. Balabekov, P. G. Romankov, E. Ya. Tarat, M. F. Mikhalev,* Operating design Conditions, of Columns with Wetted Moving Spherical Packing, J. Appl. Chem. USSR **42** (5) (1969) 1454–1458, Translated from Zhurnal Prikladnoi Khimii **42** (7) (1969) 1540–1547.
14. *M. Kito, K. Tabei, K. Murata*, Gas and Liquid Holdups in Mobile Beds under the Countercurrent Flow of Air and Liquid, Ind. Eng. Chem. Proc. Design Develop. **17** (4) (1978) 568–571, doi: https://doi.org/10.1021/i260068a030.
15. *G. V. Vunjak-Novakovic, D. V. Vukovic, H. Littman,* Hydrodynamics of Turbulent Bed Contactors 1. Operation Regimes and Liquid Holdup, Ind. Eng. Chem. Res. **26** (5) (1987b) 958–966, doi: https://doi.org/10.1021/ie00065a019.
16. *K. Soundarajan, K. Krishnaiah*, Hydrodynamics of single-stage turbulent bed contactor with downcomer, Ind. J. Chem. Technol. **6** (3) (1999) 152–160, http://nopr.niscair.res.in/handle/123456789/16916.
17. *L.-S. Fan, K. Muroyama*, Countercurrent (and Liquid-Batch) Fluidized Bed Systems, in L. S. Fan (ed.), Gas-Liquid-Solid Fluidization Engineering, Butterworth Publishers, Stoneham, USA, 1989, pp. 327–382.
18. *B. Bensebia, O. Bensebia, F. Bentahar*, Analysis of the Pressure Drop Through the Bed and Across the Supporting Grid in Type II-TBC, Experimentation and Modelling, Arab J. Sci. Eng. **41** (7) (2016) 2589–2600, doi: https://doi.org/10.1007/s13369-016-2065-y.
19. *M. Wozniack*, Pressure Drop and Interfacial Area in a column with a Mobile Bed, Int. Chem. Eng. **17** (3) (1977) 553–559.
20. *I. G. Blyakher, L. Ya. Zhivaikin, N. A. Yurovskaya*, Investigation of Hydrodynamics and Mass Transfer in Equipment with Movable Packing, Int. Chem. Eng. **7** (3) (1967) 485–490, doi: https://doi.org/10.1007/BF01150061.
21. *G. V. Vunjak-Novakovic, D. V. Vukovic, H. Littman*, Hydrodynamics of Turbulent Bed Contactors 2. Pressure Drop, Bed Expansion, and Minimum Fluidizing Velocity, Ind. Eng. Chem. Res. **26** (5) (1987a) 967–972, doi: https://doi.org/10.1021/ie00065a020.
22. *S. Ushida, C. S. Wong, C. Y. Wen*, Mechanics of a Turbulent Contact Absorber, Can. J. Chem. Eng. **55** (4) (1977) 392–396, doi: https://doi.org/10.1002/cjce.545055040.
23. *I. P. Levsh, N. I. Krainev, M. I. Niyazov*, Calculations the Pressure Drop and Heiglits of Three-Phase Fluidized Beds, Int. Chem. Eng. **8** (2) (1968a) 311–312.
24. *I. P. Levsh, N. I. Krainev, M. I. Niyazov*, Hydrodynamic Calculation of Absorbers with Fluidized Beds, Int. Chem. Eng. **8** (4) (1968b) 619–622.
25. *R. G. Barile, D. W. Meyer*, Turbulent Bed Cooling Tower, Eng. Progress Symposium Series 119 (67) (1971) 134–143.
26. *B. Z. Uysal*, Hydrodynamic and Particulate Recovery Studies in Mobile-Bed Contacting, Ph.D. Thesis, Mc-Gill Univ, 1978.
27. *M. Kito, M. Shimada, T. Sakai, S. Sugiyama, C. Y. Wen*, Performance of Turbulent Bed Contactor Gas Holdup and Interfacial Area under Liquid Stagnant Flow, in D. L. Kearns, (ed.) Fluidization Technology, ed. by, Hemisphere Publishing Co Washington, 1976b, pp. 411–429.
28. *M. Kito, M. Sawada, M. Shimada, M. Takada, T. Sakai, S. Sugiyama*, Gas holdup in a Mobile Beds with stagnant liquid Flow, Int. Chem. Eng. **16** (2) (1976c) 701, doi: https://doi.org/10.1252/kakoronbunshu.2.12.
29. *V. I. Mayak, V. I. Matrozov*, Hydraulic Resistance of Plate Columns with Fluidized Packing, Theor. Foundat. Chem. Eng. **3** (1969) 64–67.
30. *J. Tichy, A. Wong, W. J. M Douglas*, Pressure Drop in a Mobile-Bed Contactor, Can. J. Chem. Eng. **50** (1972) 215–220, doi: https://doi.org/10.1002/cjce.5450500213.
31. *M. Kito, T. Monma, Y. Kayama, T. Sakai, S. Sugiyama*, Pressure Drop and Bed Expansion in a Mobile Bed, Kagaku Kogaku Ronbunshu **2** (5) (1976a) 476–478, doi: https://doi.org/10.1252/kakoronbunshu.2.476.
32. *B. H. Chen, W. J. M. Douglas*, Liquid Holdup and Minimum Fluidization Velocity in a Turbulent Contactor, Can. J. Chem. Eng. **46** (1968) 245–249, doi: https://doi.org/10.1002/cjce.5450460406.
33. *O. P Rama, D. P. Rao, V. S. Rao*, Hydrodynamics of a Mobile Bed Contactor with Low Density Packing Particles of Different Shapes, Can. J. Chem. Eng. **61** (1983) 863–868, doi: https://doi.org/10.1002/cjce.5450610614.
34. *K. Soundarajan*, Hydrodynamics of single and multi-stage turbulent bed contactor with and without downcomer, Ph.D. Thesis, Indian Institute of Technology Madras, 1995.
35. *O. S. Balabekov, E. Ya. Tarat. P. G. Ramenkov, M. F. Mikhalev*, Hydrodynamics of Column with Wetted Fluidized Spherical Packing, J. Appl. Chem. USSR **42** (1969b) 2128–2131. Translated from Zhurnal Prikladnoi Khimii **42** (10) (1969) 2266–2270.
36. *M. L. Gimenes*, Particulate gaseous emission control using turbulent fluidized beds of mobile packings, Ph.D Thesis, Department of Chemical Engineering, Leeds, University of Leeds, 237, 1992.

37. *O. S. Balabkov, E. Ya. Tarat, P. G. Romankov, M. F. Mikhalev*, Hydrodynamic Design Calculations for Equipment with Wetted Fluidized Spherical Packing, J. Appl. Chem. USSR **42** (1969a) 1068–1074. Translated from Zhurnal Prikladnoi Khimii **44** (5) (1969) 1061–1068.
38. *A. Shabani, S. Tavosi, B. H. Shahraki*, Calculation of effective interfacial area in a Turbulent Contact Absorber, Int. J. Chem. Eng. Appl. **1** (1) (2010) 117–122, doi: https://doi.org/110.7763/IJCEA.2010.V1.20.
39. *L. Mbua Egbe,* Design and characterization of fluidized bed cooling towers, PhD thesis, Middlesex University UK, 2001, url: https://eprints.mdx.ac.uk/id/eprint/8005 (16. 11. 2021).
40. *H. Abukhalifeh, C. Mouli Madhuranthakam, R. Dhib,* Empirical models for the hydrodynamics of turbulent bed contactor with non-Newtonian liquids, (part 3), Chem. Eng. Commun. **208** (1) (2019) 1–16, doi: https://doi.org/10.1080/00986445.2019.1694914.

SAŽETAK

Zadržavanje plina u kontaktoru s turbulentnim slojem: eksperimenti i model predviđanja

Bensaber Bensebia,[a*] *Fatma Zohra Chaouche*[a] i *Soumia Kouadri Moustefai*[b]

Poznavanje zadržavanja plina važno je za razvoj trofaznih reaktora s fluidiziranim slojem. Ovaj rad bavi se proučavanjem utjecaja različitih radnih uvjeta na zadržavanje plina u kontaktoru s turbulentnim slojem tipa 2 (TBC), kao što su površinske brzine plina i tekućine, omjer masenih protoka tekućine i plina (*L*/*G*), promjer čestica i gustoća, statička visina sloja i slobodna otvorena površina potporne rešetke. Dokazan je utjecaj slobodne površine potporne rešetke (φ) na zadržavanje plina. Zadržavanje plina povećalo se na 22,92 % kad se φ smanjio s 0,82 na 0,32. Iz dobivenih eksperimentalnih rezultata (1746) razvile su se dvije korelacije za predviđanje zadržavanja plina, od kojih je jedna uključivala omjer *L*/*G*, koji je važan faktor pri dizajnu plinsko-tekućinskih kontaktora. Predviđeni rezultati zadržavanja plina podudarali su se s eksperimentalnim podatcima.

Ključne riječi
Kontaktor s turbulentnim slojem, zadržavanje plina, pad tlaka, potporna rešetka, model predviđanja

[a] *Laboratory of "Plant Chemistry-Water-Energy", Department of Process Engineering, Faculty of Technology, Hassiba Benbouali University, B.P. 151, 02 000 Chlef, Alžir*
[b] *Department of Process Engineering, Faculty of Technology, Hassiba Benbouali University, B.P. 151, 02 000 Chlef, Alžir*

Izvorni znanstveni rad
Prispjelo 30. prosinca 2021.
Prihvaćeno 19. ožujka 2022.